Research Square

Preprints are preliminary reports that have not undergone peer review.
They should not be considered conclusive, used to inform clinical practice,
or referenced by the media as validated information.

Chlormethine Treatment Effectively Targets the Tumor Microenvironment in Early-stage Mycosis Fungoides patients

Selinde S. Wind
Centre for Human Drug Research
Marie S.N. Chevalier Florquin
Leiden University Medical Center
Rianne Rijneveld
Centre for Human Drug Research
Ingrid Tomljanovic
Erasmus MC
Hendrika W. Grievink
Centre for Human Drug Research
Willem H. Zoutman
Leiden University Medical Center
Roderick C. Slieker
Leiden University Medical Center
Veerle A. Merkus
Leiden University Medical Center
Yalçin Yavuz
Centre for Human Drug Research
Mick van Schaick
Centre for Human Drug Research
Naomi Klarenbeek
Centre for Human Drug Research
Tessa Niemeyer - van der Kolk
Centre for Human Drug Research
Manon A.A. Jansen
Centre for Human Drug Research
Anne M.R. Schrader
Leiden University Medical Center
Patty M. Jansen
Leiden University Medical Center
Noel F.C. de Miranda

Leiden University Medical Center
Marieke E. Ijsselsteijn
Leiden University Medical Center
Rein Willemze
Leiden University Medical Center
Koen D. Quint
Leiden University Medical Center
Robert Rissmann
rrissmann@chdr.nl

Centre for Human Drug Research
Maarten H. Vermeer
Leiden University Medical Center

Research Article

Keywords:

Posted Date: November 16th, 2026

DOI: https://doi.org/10.21203/rs.3.rs-11562688/v1

License: This work is licensed under a Creative Commons Attribution 4.0 International License.
Read Full License

Additional Declarations: No competing interests reported.

Chlormethine Treatment Effectively Targets the Tumor Microenvironment in Early-stage Mycosis Fungoides patients

Selinde S. Wind[1–3], Marie S.N. Chevalier Florquin[2], Rianne Rijneveld[1], Ingrid Tomljanovic[4], Hendrika W. Grievink[1], Willem H. Zoutman[2], Roderick C. Slieker[5], Veerle A. Merkus[2], Yalçin Yavuz[1], Mick van Schaick[1], Naomi Klarenbeek[1], Tessa Niemeyer - van der Kolk[1], Manon A.A. Jansen[1], Anne M.R. Schrader[3], Patty M. Jansen[3], Noel F.C. de Miranda[3], Marieke E. Ijsselsteijn[3], Rein Willemze[2], Koen D. Quint[2], Robert Rissmann[1,2,6], and Maarten H. Vermeer[2]

The Next Generation ImmunoDermatology (NGID) Consortium*

[1]Centre for Human Drug Research, Dermatology, Leiden, The Netherlands; [2]Leiden University Medical Center, Dermatology, Leiden, The Netherlands; [3]Leiden University Medical Center, Pathology, Leiden, The Netherlands; [4]Erasmus Medical Center, Rotterdam, The Netherlands; [5]Leiden University Medical Center, Medical Oncology, Leiden, The Netherlands; and [6]Leiden Academic Centre for Drug Research, Division of BioTherapeutics, Leiden, The Netherlands.

Main text: 3988 words, Abstract: 249 words, Title: 112 including spaces, Figures: 7, Number of references: 45

Corresponding authors:

Prof. Robert Rissmann, PhD, Research Director, Centre for Human Drug Research, Zernikedreef 8, 2333CL Leiden, The Netherlands; rrissmann@chdr.nl

Prof. Maarten Vermeer, MD, PhD, Leiden University Medical Center, Department of Dermatology, Leiden University, Albinusdeef 2, 2300ZA Leiden, Leiden, The Netherlands, m.h.vermeer@lumc.nl.

Data sharing statement: Imaging mass cytometry, flow cytometry and proteomic data may be found in a data supplement available with the online version of this article. The study protocol and all data and/or code generated during the study are available from the corresponding author upon reasonable request and in line with data sharing stipulations under GDPR.

*A complete list of the members of the Next Generation ImmunoDermatology Consortium appears in the ‘’Appendix’’.

Key points

1. Chlormethine response in early-stage MF is associated with baseline cytotoxic immune environment and treatment-induced immune activation.
2. Responders exhibit T cell clonal contraction and reduction of immunosuppressive programs, while non-responders retain a tumor tolerant architecture.

ABSTRACT

Topical chlormethine is an established skin-directed therapy for early-stage mycosis fungoides (MF), yet treatment response is heterogeneous and treatment-associated dermatitis is common, suggesting incompletely defined mechanisms within the tumor microenvironment (TME). We investigated how chlormethine remodels the MF TME and which baseline features associate with clinical response. In an exploratory, prospective, open-label study, 21 early-stage MF patients applied chlormethine gel for 16 weeks; 17 were analyzed. At baseline, paired lesional and non-lesional suction blister fluid and biopsies were collected; the same lesion was resampled after treatment, and electively during dermatitis. Healthy controls (n=10) provided baseline samples. Immune profiling integrated flow cytometry, targeted proteomics, imaging mass cytometry and TCRβ sequencing to characterize cellular, proteomic, and clonal dynamics. Chlormethine induced heterogeneous clinical improvement at week 16, and dermatitis duration correlated with response magnitude. Baseline analyses identified an immune-reactive TME in responders, enriched for activated cytotoxic T cells in lesional versus non-lesional skin. Dermatitis samples demonstrated activated immune infiltrates and proteomic signatures of inflammatory cell recruitment, marking a treatment-associated immune-activation phase followed by clonal and inflammatory contraction—including reductions in dominant T-cell clones, aberrant T cells, regulatory T cells, and immunosuppressive mediators. Longitudinal analyses indicates coordinated modulation of interferon pathways, cytotoxic effector signatures, and checkpoint signaling, identifying cytotoxic interferon-associated immunity as a principal driver of response. These findings support a biphasic mechanism of action—direct tumor cytotoxicity and immune-mediated TME remodeling—and provide rationale for immune-based stratification in early-stage MF. This trial was registered at www.clinicaltrials.gov as #NCT05303480 and EudraCT as #2021-001576-41.

INTRODUCTION

Cutaneous T-cell lymphomas (CTCLs) represent a heterogeneous group of primary cutaneous T-cell lymphomas characterized by malignant, skin-homing T lymphocytes. Mycosis fungoides (MF) is the most common subtype of CTCL, accounting for 50-80% of cases with an incidence of 0.3–0.9 per 100,000 person-years [1]. Early-stage MF typically presents with patches and plaques and follows an indolent yet slowly progressive clinical course, advancing from patches and plaques to tumor stage disease, with disease stage correlating directly with prognosis and survival [2].

Early-stage MF remains largely skin-confined and is addressed by skin-directed therapies including topical steroids, light therapy and topical chlormethine [3]. Topical chlormethine (mechlorethamine), a bifunctional alkylating agent, has been known for decades in MF management [4–8]. Clinical studies have reported overall response rates ranging from 58.5% to 81.6%, with complete response (CR) rates of 13.8%–22.5%. However, therapy discontinuation rates attributable to treatment-related dermatitis have been documented in 4.1%–20.3% of patients. The mean time to achieve peak clinical response has been reported to vary between 10 and 18 months [9–13]. This study was designed to include 16 weeks of chlormethine treatment based on the pharmacodynamic response rate previously published [9], demonstrating 46% of patients using chlormethine gel with a partial to complete response at 16W. This timespan was chosen to capture early pharmacodynamic immune remodeling in approximately half of the patients, which we postulated not only precedes but also drives the attainment of maximal clinical response. Despite its established efficacy, the heterogeneity of response, the delayed attainment of maximal effect, and the frequent occurrence of cutaneous adverse reactions may limit use of chlormethine treatment [14–16].

In vitro studies using T cells extracted from MF skin lesions established that chlormethine induces DNA double-stranded breaks and suppressed expression of DNA-repair genes leading to apoptosis [8,17,18]. While its DNA cross-linking properties have been well-documented as the primary mechanism of action, recent translational work suggests that immunomodulatory mechanisms may contribute to clinical response in alkylating chemotherapeutics [8,19,20], a concept that has also been proposed for chlormethine therapy [21]. Of particular interest, therefore, is the nature and underlying biology of the cutaneous adverse reactions associated with topical chlormethine [5,15,16]. Although these are currently labelled as irritant or allergic contact dermatitis, an intriguing possibility remains that the inflammatory response may contribute to therapeutic efficacy. Hence, the immunomodulatory effects of chlormethine leading to a pro-inflammatory, cytotoxic milieu could be an integral part of the therapeutic effect of chlormethine therapy [22–25].

In this prospective translational study, we investigated the effects of topical chlormethine therapy on the tumor microenvironment (TME) in early-stage MF and correlated findings with clinical response.

METHODS

Study design and treatment

An exploratory, open-label interventional study was conducted in patients with early-stage MF (stage IA–IB) and healthy controls (HC) at the Centre for Human Drug Research (Leiden, the Netherlands) between October 2021 and December 2022. The study was approved by an independent medical ethics committee and conducted in accordance with the Declaration of Helsinki. All participants provided written informed consent. The trial was registered in EudraCT (2021-001576-41) and ClinicalTrials.gov (NCT05303480).

After a washout period of CTCL-related therapies, patients applied topical chlormethine gel (0.016%) to all MF lesions excluding the face. Treatment started with three applications per week for four weeks and was escalated to once-daily application from week 5 to week 16. Study design, detailed treatment schedules and rescue medication are provided in Figure 1 and Table S1.

Participants

MF patients aged 18–75 years with a histologically confirmed early-stage MF and at least one patch or plaque lesion ≥6 cm were eligible for this study. Patients could only be included after topical CTCL treatments had been discontinued for 8 weeks and systemic CTCL treatments had been discontinued for 10-18 weeks, depending on the time required to reach 5 half-lives, prior to the baseline week 0 visit. Key exclusion criteria included recent use of antibiotics, prior chlormethine treatment, clinically significant comorbidities, or the need for systemic anti-cancer therapy.

HC were approximately matched with the patient cohort in terms of age, sex, and target location, as outlined in Table 1. Exclusion criteria for healthy volunteers included the presence of significant skin disease, use of topicals on the target area in the past two weeks and a history of hypertrophic scarring. Full inclusion and exclusion criteria for MF patients and HC are listed in Tables S2–S3.

Clinical response, compliance, safety and skin assessments

Disease severity was assessed using the modified Severity Weighted Assessment Tool (mSWAT). A predefined target lesion was longitudinally evaluated using the Composite Assessment of Index Lesion Severity (CAILS) [26]. Treatment response was assessed using modified CAILS (mCAILS), excluding pigmentation scores to minimize confounding by post-inflammatory hyperpigmentation. All assessments were performed by one of two trained investigators.

Safety and tolerability were evaluated through adverse event monitoring, laboratory assessments, vital signs, and Local Irritation Grading Scale (LIGS). Target lesions and contralateral non-lesional control skin

were assessed at baseline and after 4, 8, 12, and 16 weeks of treatment for clinical response, and using standardized clinical photography and laser speckle contrast imaging (LSCI) [27–30].

Suction blisters and 4-mm punch biopsies were collected from lesional and non-lesional skin at baseline. After 16 weeks of treatment, repeat samples were obtained from the target lesion only.

Proteomic, immunophenotypic, tissue analyses and statistics

Blister fluid was analyzed using targeted proteomic panels assessing inflammatory and immuno-oncology-related proteins. Cellular pellets were subjected to flow cytometry-based immunophenotyping. Skin biopsies were processed for histology, immunohistochemistry, imaging mass cytometry (IMC), and a subset of 8 biopsies (4 responders and 4 non-responders) for high-throughput T-cell receptor β sequencing (TCRβ-seq) using established protocols. Detailed methodologies, antibody panels, gating strategies, IMC phenotype annotation, T-cell receptor sequencing and are provided in the Supplemental Methods, Table S4–S6 and Figure S1–S2. Statistical testing was performed per protocol and is described in detail in the Supplemental.

RESULTS

Chlormethine induces heterogeneous early clinical responses and treatment-associated dermatitis correlates with treatment response by mCAILS

Twenty-one patients with MF stage IA–IB and eleven HC were enrolled, and all patients were treated; nineteen MF patients (90.5%) completed the 16-week study. Two patients withdrew early due to persistent dermatitis reactions; they were included for analysis using last-observation-carried-forward. Four patients were excluded from analysis due to differential disease subtypes, a total of 17 patients (81.0%) and 10 HC (90.9%) were analyzed (N=4 excluded from the analysis set due to differential MF subtypes, see STROBE flow chart Supplementary Figure S3). Patients were treated with chlormethine gel on a mean treated BSA of 11.9% (range 2–79%). Patient, baseline, and treatment characteristics are provided in Table 1.

After 16 weeks, three patients (17.6%) demonstrated a fast clinical response (FR), reflected by a ≥70% mean reduction in mCAILS (Δμ−10.8, 95%CI: 3.04-20.96, p=0.029) compared to baseline. Four patients (23.5%) showed an intermediate response (IR, ≥50–70% mCAILS mean reduction, Δμ −9.1, 95%CI: 2.94-16.26, p=0.016), and four (23.5%) a slow response (SR, ≥20–50% mCAILS mean reduction, Δμ −4.7, 95%CI: 1.47-8.03, p=0.019). All responder groups had a significantly greater mean reduction in mCAILS score compared to non-responders (NR) at week 16 (n=6, 35.3%, Figure 2A–B). When responders were analyzed as a single group (n=10), mean mSWAT score significantly decreased after treatment

(μ±σ,14.10±21.96 vs 11.20±20.03, p=0.015). In contrast, among non-responders (n=6), there was no significant evidence for a change (9.00±4.00 vs 8.50±4.46, p=0.636). Between responder-group comparison did not demonstrate statistically significant evidence of a difference.

Adverse events (AEs) occurred in 19 patients (90.5%) and were exclusively mild (n=25) or moderate (n=16, Table S7). No serious AEs or deaths were observed. Dermatitis was the most common AE (Table S8, indicated as ASR), occurring in 15 patients (71.4%). No clinically relevant changes in laboratory parameters, ECG or vital signs were detected.

Almost all responders (90.9%) experienced dermatitis reactions with a mean duration of 21.3 days, compared to only 33.3% of non-responders with a mean duration of 2.8 days. Treatment response, measured by change in modified Composite Assessment of Index Lesion Severity (mCAILS) from baseline, was strongly correlated with dermatitis duration (days) in the treated skin (r=0.60, 95%CI: 0.13-0.85, p=0.02), Figure 2C.

Baseline MF lesions show an inflamed immune infiltrate relative to non-lesional skin

Detailed characterization of the baseline TME from blister fluid using flow cytometry in patients with stage IA-IB mycosis fungoides, showed significantly elevated immune cell populations in lesional versus non-lesional skin ($p<0.01$), including total T-lymphocytes ($p<0.01$), $CD4^+$ T-lymphocytes ($p<0.01$), aberrant $CD4^+CD26^-$ T-lymphocytes ($p<0.01$), activated $CD4^+HLA\text{-}DR^+$ effector T-lymphocytes ($p=0.01$), $CD8^+$ cytotoxic T-lymphocytes ($p<0.01$), activated $CD8^+HLA\text{-}DR^+$ cytotoxic T-lymphocytes ($p<0.01$), $CD14^-CD16^-$ dendritic cells ($p<0.01$) and $CD68^+$ histiocytes ($p<0.01$, Figure S4). This baseline characterization provides important context for response-associated remodeling to topical chlormethine treatment.

Baseline cytotoxic TME distinguishes responders from non-responders

At baseline, responders (fast, intermediate and slow taken together) demonstrated a significantly higher prevalence of activated cytotoxic T-cells in lesional skin (median=1284, interquartile range (IQR): 142–3395) compared with non-lesional skin (mdn=389, IQR:270 – 736, p-adjusted=0.023), a distinction not observed in non-responders (Figure 2D). This observation suggests that the pre-existing composition of the immune infiltrate may contribute to therapeutic efficacy of topical chlormethine treatment. Complementary to the blister fluid analysis, we performed IMC on lesional biopsies obtained before and after 16 weeks of treatment (Figure 4). At baseline, responders showed a marginal increase in total immune cells compared to non-responders, consistent with the blister fluid findings; however, this difference could not be attributed to any specific cell population (Figure 4, S5–6). Furthermore, no differences in cellular spatial interactions were detected in the tissue at baseline.

Responders exhibit reduction of dominant T-cell clones after chlormethine treatment

Chlormethine treatment-induced changes in tumor burden and infiltrating T cells were confirmed in 4 responders compared to 4 non-responders using high-throughput T-cell receptor sequencing (TCRβ-seq). Data from one responder were excluded due to insufficient T-cell numbers. At baseline, lesions exhibited high T-cell diversity, ranging from 81 to 895 unique clones. The majority of clones were transient, with only 0–57 shared clones detected between paired baseline and treated samples (Figure S7). In responders, the diversity of T-cell clones decreased from baseline (ranging from 211 to 895 unique clones, Figure 3A) to treated samples, with a marked reduction in the abundance of top T-cell clones (Figure 3B and S7). In contrast, non-responders at week 16 showed either no change or an increase in these clonal populations, suggesting that the combination of direct cytotoxicity and immunomodulatory effects may be important for optimal clinical response. Combined, the fast and intermediate responders showed a consistent reduction in the contribution of the top-10 most abundant T-cell clones following treatment (Figure S7). In contrast, non-responders showed stable or increased dominance of these clones, indicating persistence of clonal T-cell expansion despite treatment (Figure 3C and S7).

Clinical response is accompanied by contraction of inflammatory and immunosuppressive cellular programs

When comparing responders to non-responders on treatment, IMC visualization reveals a marked decrease in immune infiltrate in treated biopsies (Figure 4A). This observation is corroborated by quantitative analysis, which shows stable or increased total immune cell counts in non-responders, whereas responders demonstrate a decrease in immune cells after 16 weeks of treatment (Figure 4B). This pattern does not appear to be driven by a specific immune cell type, as a similar trend is recognized across immune cell populations (Figure 4C-D).

Blister fluid of responders exhibited a significant median decrease in CD3+CD4+CD26- aberrant T cells (mdn= 1298 absolute cells, IQR 423–1684 vs mdn=133, IQR 16–433, p_{adj}=0.035) and regulatory T cells (Tregs, mdn=1474, IQR 882–2454 vs mdn=160, IQR 56–510, p_{adj}=0.035), supporting conciliation of the previously immunosuppressive cellular microenvironment. Additionally, responders showed a significant median reduction in total lymphocytes (mdn=9237, IQR 5358–13148 vs mdn=1021, IQR 294–2885, p_{adj}=0.020), dendritic cells (mdn=1172, IQR 506–1547 vs mdn=90, IQR 20–273, p_{adj}=0.035), histiocytes (mdn=36, IQR 16–178 vs mdn=3, IQR 0–11, p_{adj}=0.035), activated CD4+ lymphocytes (mdn=970, IQR 338–2519 vs mdn=155, IQR 46–639, p_{adj}=0.035), CD8+ regulatory T cells (mdn=1040, IQR 421–4155 vs mdn=98, IQR 48–237, p_{adj}=0.035) and cytotoxic T cells (mdn=2318, IQR 465–9507 vs mdn=315, IQR 78–969, p_{adj}=0.035, Figure 5), reflecting resolution of the inflammatory infiltrate after response. In contrast, in non-responders at week 16 we observed no evidence to show significant reductions in aberrant T cells, regulatory T cells, total lymphocytes or (activated) cytotoxic lymphocytes, in line with the persistent T cell clones observed in TCRβ-seq data.

Blister-fluid proteomics reveals extensive baseline lesional dysregulation and remodeling after chlormethine.

To characterize the soluble immune landscape of the MF TME and its modulation by chlormethine treatment, targeted proteomic profiling of suction blister fluid (Olink® Target 96 Immuno-Oncology and Inflammation panels) was performed, containing 184 target proteins. At baseline, lesional MF blister fluid showed a broad disease-associated soluble signature relative to both healthy control skin (67 unique significant proteins after deduplication across both panels) and paired non-lesional skin (70 unique significant proteins), consistent with an interferon-driven and cytotoxic, chronically inflamed lesional microenvironment (Figure 6B, Table S9, Figure S8A–B). Most notably, high levels of IFN-γ, IL12, CD40, CD244, CXCL9, CXCL10, CXCL11 and PD-L1 characterized MF stage Ia-Ib lesions (Figure 6B). In contrast, non-lesional skin differed only modestly from healthy controls (6 unique proteins, $p_{adj}<0.05$), indicating that the inflammatory signal was largely lesion-restricted (Figure S8C). Following 16 weeks of chlormethine treatment, lesional blister fluid demonstrated significant remodeling relative to baseline, comprising 29 unique proteins ($p_{adj}<0.05$, Figure 6A) supporting measurable pharmacodynamic shifts in the soluble TME at this early time point. This shift was predominantly a reduction in inflammatory and cytotoxic mediators such as GZMB, IFN-γ, CXCL9, CXCL11, MCP-3, IL12 and CCL20, with only IL13, IL7 and CCL23 expression increasing after 16 weeks of treatment (Figure 6A). Notably, most proteins decreased toward non-lesional levels, but did not fully reach them (Figure 6B), consistent with partial normalization of the soluble microenvironment.

Higher baseline immune activity in blister-fluid proteomics indicates response to chlormethine

Importantly, baseline proteomic profiles separated responders from non-responders, with 39 proteins differing between them, of which the 11 most significant ones ($p_{adj}<0.01$) are shown in Figure 6C. Responders exhibited a higher baseline expression of proteins involved in T-cell activation and co-stimulation (GZMH, CD27, CD28, CD83, TNFRSF4, TNFRSF9, and SLAMF1), immune checkpoint regulation (ICOSLG, PD-L1, PD-L2), and tumor survival, proliferation and migration (CCL28, CXCL12, MMP-1, TNF and TNFRSF21; Figure 6C and S9A).

Treated samples from responders exhibited a comparatively restricted soluble profile, whereas non-responders retained a higher abundance of a broad set of immune and inflammation-associated mediators (with the 27 most significant ones at adjusted $p<0.01$ shown in Figure 6D), consistent with persistence of an activated, checkpoint- and chemokine-rich milieu in lesions lacking clinical improvement (Figure S9B). Protein-protein interaction (PPI) network analysis of treated samples showed high expression of hub proteins pivotal in negative regulation of activated T cell proliferation and cytokine/cytokine receptor interactions in non-responders, consistent with persistent immune dysregulation (Figure S9E). Principal

component analysis suggested a continuum of treated inflammatory states, aligning with graded clinical response rather than a strictly binary responder phenotype (Figure 6E).

Dermatitis samples display a distinct, inflammation-high soluble state that differs from treated lesions

We explored the biological basis of chlormethine-induced dermatitis using IMC analyses and suction blister fluid proteomics. IMC analyses showed changes in key immune cell phenotypes during chlormethine-induced dermatitis reactions (Figure 7A–B). In our IMC cohort, 4 out of 5 dermatitis reactions occurred in responders. Among these 5 patients, cellular peaks were observed in relative abundance coinciding with dermatitis events (Figure 7B) and subsequently declined in follow-up biopsies after 16 weeks of treatment. The increase in relative abundance is heterogeneous and, in these data, not driven by a specific cell type. Although dermatitis is associated with an overall rise in cellular abundance, the contributing cell populations differ between patients in this cohort.

Suction blister fluid obtained during dermatitis reactions (n=7 from 5 patients) was compared with paired lesional baseline and lesional treated samples from the same patients. Dermatitis-associated blister fluid represented an amplified inflammatory and cytotoxic state, with 21 unique proteins ($p_{adj}<0.05$) significantly elevated in expression relative to baseline lesional blister fluid. This included amongst others CCL11, CCL19, CCL23, TNFβ, TNFSF14, KLRD1, CD8A and GZMA, while only ARG1 expression was reduced (Figure 7C). Dermatitis blister fluid likewise diverged substantially from treated lesional fluid (54 unique proteins, $p_{adj}<0.05$), the large majority of which were enriched during dermatitis relative to the post-treatment state, including IFN-γ, GZMA, GZMB, GZMH, IL6, CCL19, CCL20, CXCL11 and TNF. (Figure 7D). Notably, the dermatitis soluble profile partially overlapped with the baseline lesional inflammatory signature but was distinguished by a markedly amplified cytotoxic signature, while remaining clearly separable from the treated responder state (Figure 7E). This supports the interpretation that dermatitis reflects a phase of amplified immune activation rather than a simple continuation of treated normalization. These findings are consistent with the broader biphasic model observed across cellular and clonal readouts, in which effective chlormethine treatment is associated with an early activation state (often clinically manifesting as dermatitis) followed by contraction and partial normalization of the soluble inflammatory milieu in responders.

DISCUSSION

In Mycosis fungoides (MF) is a strong need for mechanistic insight to optimize treatment strategies. Chlormethine gel is an established skin-directed therapy in early-stage MF, yet interpatient variability in response and frequent treatment-associated dermatitis suggest that its mechanism of action is incompletely understood, hampering its full potential. Notably, the dysfunctional skin barrier associated with MF and dermatitis may itself represent an underlying factor that modulates drug penetration and local immune

activation, further contributing to the heterogeneity observed across patients [31]. In this study, we define the impact of chlormethine on the multi-immune landscape of the TME and demonstrate that clinical response is closely linked to cytotoxic immune activation.

Prior studies in cutaneous lymphomas have shown that early-stage MF lesions may harbor active $CD8^+$ T-cell infiltrates and that increased cytotoxic T-cell abundance correlates with improved survival [32–35]. Consistent with these observations, chlormethine treatment was associated with a pronounced cytotoxic inflammation in responding patients in our cohort. At baseline, responders exhibited higher frequencies of activated cytotoxic T cells and increased expression of activation- and checkpoint-associated proteins (CD27, CD28, CD83, SLAMF1, ICOSLG, PD-L1), indicating a pre-existing inflamed and immune-reactive milieu. During treatment, responders demonstrated contraction of dominant T-cell clones and reductions in aberrant T cells and regulatory T cells. Additionally, chlormethine treatment decreased levels of immunosuppressive mediators (including ARG1, TGF-α, CD244, LAMP3, IL-13 and IL-33) and inflammatory chemokines and cytokines, (e.g., IFN-γ, CXCL9 and CXCL10) over time. These findings support a model in which chlormethine amplifies an interferon-associated cytotoxic response that contributes to tumor regression.

Our longitudinal TCRβ-seq analyses extend these observations by demonstrating that clinical improvement can coincide with contraction of dominant lesional T-cell clones, supporting a reduction in tumor-associated clonal burden. This is clinically meaningful, as persistent malignant clonotypes have been linked to lesion recurrence and incomplete disease control in prior work defining the “clone-ablative” potential of skin-directed therapies: O’Malley and colleagues showed that low-dose radiotherapy effectively eradicated or markedly reduced the malignant clone in most lesions, whereas topical corticosteroids produced clinical improvement despite sustained clonal persistence—a feature that predicted recurrence [36]. Together, these findings underscore that molecular clearance of dominant malignant clones may represent an important determinant of durable lesion control and highlight the value of incorporating clonal metrics alongside clinical and immunologic endpoints when evaluating response to chlormethine.

Previous studies have demonstrated that alkylating agents exert immunomodulatory effects in addition to direct cytotoxicity [37–39]. A key observation in our study is the biphasic immune trajectory in responders: initial immune activation—characterized by increased cytotoxic activity and inflammatory signaling— was followed by contraction of inflammatory mediators and lymphocyte subsets, including activated cytotoxic T cells, alongside downregulation of 42 proteins linked to checkpoint signaling and chronic inflammation (e.g. PD-L1, FASLG, granzymes, CD40/CD40L). This contraction phase coincided with clinical improvement and restoration towards a more balanced cellular composition of the skin, suggesting that clinical improvement reflects both immune engagement and subsequent reduction of the cutaneous immune composition to a level of non-lesional skin.

We observed marked heterogeneity in treatment response, consistent with previous studies reporting a relatively slow onset of action and a mean time to peak response of approximately 10–18 months [9–13].

Responders (FR, IR, SR combined) displayed abundant activated cytotoxic T cells and activation-associated proteins at baseline, whereas non-responders at week 16 had limited pre-existing cytotoxic signatures. These data indicate that the tempo of lesion regression is shaped by the underlying immune environment. In contrast, non-responders exhibited persistence of immunosuppressive protein signatures during treatment, supporting the concept that therapeutic outcome depends on the capacity of the TME to mount an effective cytotoxic response.

Dermatitis is a common adverse event, occurring in 4.1%–20.3% of patients treated with chlormethine [9–13], and is often interpreted as allergic in nature, leading to premature discontinuation [16]. Our data challenge this interpretation. Treatment-associated dermatitis linked with heightened cytotoxic and interferon-associated activation and mirrored the inflammatory response observed in responding lesions. These cellular and proteomic patterns suggest that dermatitis extends beyond purely irritant or allergic mechanisms and may reflect treatment-induced immune activation implicated in anti-tumor immunity, which may in turn contribute to therapeutic efficacy. These data support continuing chlormethine through manageable dermatitis with supportive care and dose adjustment rather than treatment discontinuation.

A key methodological strength of this study is the use of suction blister fluid to sample the cutaneous immune microenvironment in MF patients. While suction blistering has been validated as a minimally invasive technique to capture skin-resident immune cells and soluble mediators in inflammatory dermatoses [40–43], its application to assess the TME in cutaneous lymphoma has not been previously reported. By assimilating suction blister–derived protein and cellular data with IMC of tissue biopsies, we established a multi-modal framework that bridges spatial architecture with functional immune profiling — enabling simultaneous assessment of the TME at complementary levels of resolution.

Several limitations should be considered when interpreting these data. Although suction blisters provide a representative snapshot of the dermal–epidermal immune compartment, cell-type-specific migration into blister fluid may not uniformly reflect the composition of the underlying tissue. Larger or tissue-resident cells, as well as cells tightly embedded in the stromal matrix, may be underrepresented relative to highly motile lymphocyte populations. Future studies combining suction blister sampling with single-cell transcriptomics of matched biopsies could further delineate the extent to which blister-derived profiles recapitulate the full complexity of the MF microenvironment. Additionally, interpretation of the dermatitis-associated immune signatures warrants caution, given that the dermatitis subgroup comprised only five patients and therefore has limited generalizability and should be considered hypothesis-generating. Furthermore, IMC and proteomic analyses offer static cross-sectional assessments rather than continuous temporal resolution, making it likely that transient activation states and evolving inflammatory trajectories remain incompletely represented. Establishing the clinical relevance of these dermatitis-associated signatures will require confirmation in larger cohorts with serial sampling across the evolution of the inflammatory response. Lastly, in this exploratory study we evaluated early pharmacodynamic immune

remodeling at 16 weeks of treatment; clinical responses emerging beyond this time point were not assessed.

By integrating multi-omics using flow cytometry and proteomics of suction blister fluid, IMC and T-cell receptor sequencing of skin biopsies, this study provides a high-dimensional, protein-level characterization of immune dynamics during chlormethine therapy. Prior reports have suggested shifts from Th1- to Th2-skewed responses in MF [22,38,44]; our longitudinal analyses may extend these findings by indicating coordinated modulation of interferon pathways, cytotoxic effector signatures, and checkpoint signaling, identifying cytotoxic interferon-associated immunity as a principal driver of response.

In conclusion, our results demonstrate that chlormethine treatment in early-stage MF reduces immune suppression and is associated with induction and modulation of a cytotoxic immune response within the TME. A pre-existing activated cytotoxic milieu predicts more rapid and pronounced clinical lesion improvement by mCAILS, whereas tumor-promoting environments are associated with resistance. These findings support a dual mechanism of action for chlormethine i) direct tumor cytotoxicity and ii) immune-mediated reshaping of the TME [7,45]. We provided a mechanistic rationale for prospective biomarker-stratified trials in which baseline cytotoxic T-cell signatures and activation-associated protein expression could guide MF patient selection for chlormethine therapy.

ACKNOWLEDGEMENTS

The authors express their gratitude to all patients and healthy control participants involved in this study and to the patient advocacy group Stichting Huidlymfoom.

This research was partially funded by Helsinn and Recordati Rare Diseases, they had no role in gathering, analyzing or interpreting the data, and no role in writing the manuscript or in the decision to publish the results. S.S.W. is a PhD candidate at the Centre for Human Drug Research and Leiden University Medical Center, M.C. is a PhD candidate at Leiden University Medical Center. This work is submitted in partial fulfillment of the requirement for the PhD.

FUNDING

This investigator-initiated study was funded by CHDR and supported by Recordati Rare Diseases/Helsinn. This publication is part of the project Next Generation ImmunoDermatology (NGID) NWA.1389.20.182 of the NWA research programme ‘Research along Routes by Consortia (ORC)’, which is financed by the Dutch Research Council (NWO).

AUTHORSHIP CONTRIBUTIONS

Contribution: S.S.W., T.N.v.d.K., and R.R. study design; S.S.W., R.B., M.v.S., T.N.v.d.K., M.A.A.J., N.K., and R.R. clinical study conduct; S.S.W., M.S.N.C., I.T., H.W.G., W.H.Z., R.C.S., V.A.M., A.M.R.S., P.J., N.F.C.d. M., and M.E.I. methodology; S.S.W, M.S.N.C., I.T., W.H.Z. data analysis; S.S.W., R.B., M.v.S., K.D.Q., and M.H.V. participant recruitment; S.S.W. writing original draft preparation; M.S.N.C., R.W., M.E.I., Y.Y., I.T., R.W., R.R. and M.H.V. writing, review and editing; S.S.W., M.S.N.C., I.T., W.H.Z., and R.S. visualization; K.D.Q. and M.H.V. clinical supervision; All authors have read and agreed to the published version of the manuscript.

Correspondence: Robert Rissmann, Centre for Human Drug Research, Dermatology, Leiden, The Netherlands, e-mail: rrissmann@chdr.nl. Maarten Vermeer, Leiden University Medical Center, Dermatology, Leiden, The Netherlands, e-mail: m.h.vermeer@lumc.nl.

Conflict-of-interest disclosure: The authors declare no competing financial interests.

APPENDIX

Collaborators (PubMed citation) NGID consortium: Rob Vreeken, Maastricht University; Eva Cuypers, Maastricht University; Boudewijn Lelieveldt, Leiden University Medical Center; Abdoel El Ghalbzouri, Leiden University Medical Center; Hanna Niehues, Radboud University Medical Center; Ellen van den Bogaard, Radboud University Medical Center; Tom Ederveen, Radboud University Medical Center; Peter A.C. 't Hoen, Radboud University Medical Center; Els van der Pool, HAN University of Applied Sciences; Nanda Olde, HAN University of Applied Sciences; Debra Trampe, HAN University of Applied Sciences; Lisanne Wezendonk, Leiden University Medical Center; Johan Westerhuis, University of Amsterdam; Huma Shehwana, University of Amsterdam; Jimmy Bakker, Perimed; Matthijs Moerland, CHDR; Femke van Wijk UMC Utrecht; Arjan Schoneveld UMC Utrecht; Victor van der Valk, Leiden University Medical Center; Igor Radanović CHDR; Peter van den Broek, HuidNederland; Bernd Arents, VCME; Ton de Leeuw, Stichting Huidlymfoom; Tom Ederveen, Radboud UMC; Peter Bram 't Hoen, Radboud UMC; Annemarie Sluijmers, Nationale vereniging voor mensen met lupus, APS, sclerodermie en MCTD; Bernd Arents, Vereniging voor Mensen met Constitutioneel Eczeem; Mieke de Leeuw, Stichting Huidlymfoom; Ton de Leeuw, Stichting Huidlymfoom; Douwe Vellinga, Alrijne Hospital Leiderdorp; Stephan Weidinger, University Hospital Kiel Schleswig Holstein; Sandrine Dubrak, Medical University of Innsbruck; Yang Li, Helmholtz Centre for Infection Research; Maurice Steensel, Nanyang Technological University, Singapore; Martina Marchetti-Deschmann, Technical University Wien. Matthijs Moerland, Centre for Human Drug Research; Michelle Osse, Centre for Human Drug Research, Jacobus Bosch, Centre for Human Drug Research, Koos Burggraaf, Centre for Human Drug Research.

REFERENCES

1. Willemze R, Cerroni L, Kempf W, Berti E, Facchetti F, Swerdlow SH, et al. The 2018 update of the WHO-EORTC classification for primary cutaneous lymphomas. Blood. 2019;133(16):1703–14. doi:https://doi.org/10.1182/blood-2018-11-881268

2. Mourad A, Gniadecki R. Overall Survival in Mycosis Fungoides: A Systematic Review and Meta-Analysis. Journal of Investigative Dermatology. 2020 Feb 1;140(2):495-497.e5. doi:10.1016/j.jid.2019.07.712 PubMed PMID: 31465745.

3. Latzka J, Assaf C, Bagot M, Cozzio A, Dummer R, Guenova E, et al. EORTC consensus recommendations for the treatment of mycosis fungoides/Sézary syndrome – Update 2023. European Journal of Cancer. Elsevier Ltd; 2023. doi:10.1016/j.ejca.2023.113343 PubMed PMID: 37890355.

4. Garcia-Saleem TJ, Stonesifer CJ, Khaleel AE, Geskin LJ. Management of mycosis fungoides with topical chlormethine/ mechlorethamine gel: A columbia university cutaneous lymphoma center experience. Acta Derm Venereol. 2021 Sep 1;101(9). doi:10.2340/00015555-3911 PubMed PMID: 34436621.

5. Kim EJ, Guitart J, Querfeld C, Girardi M, Musiek A, Akilov OE, et al. The PROVe Study: US Real-World Experience with Chlormethine/Mechlorethamine Gel in Combination with Other Therapies for Patients with Mycosis Fungoides Cutaneous T-Cell Lymphoma. Am J Clin Dermatol. 2021 May 1;22(3):407–14. doi:10.1007/s40257-021-00591-x PubMed PMID: 33656660.

6. Guenova E, Ortiz-Romero PL, Poligone B, Querfeld C. Mechanism of action of chlormethine gel in mycosis fungoides. Journal of the European Academy of Dermatology and Venereology. 2023;37(9):1739–48. doi:10.1111/jdv.19237 PubMed PMID: 37262305.

7. Ardigò M, Nikbakht N, Teoli M, Gleason L, Crisan L, Querfeld C. Chlormethine gel in combination with other therapies for treatment of mycosis fungoides: a review with patient cases. Front Med (Lausanne). 2023;10:1308491. doi:10.3389/fmed.2023.1308491 PubMed PMID: 38274457.

8. Lawley PD, Brookes P. Molecular mechanism of the cytotoxic action of difunctional alkylating agents and of resistance to this action. Nature. 1965 May;206(983):480–3. doi:10.1038/206480a0 PubMed PMID: 5319105.

9. Querfeld C, Scarisbrick JJ, Assaf C, Guenova E, Bagot M, Ortiz-Romero PL, et al. Post hoc Analysis of a Randomized, Controlled, Phase 2 Study to Assess Response Rates with Chlormethine/Mechlorethamine Gel in Patients with Stage IA–IIA Mycosis Fungoides. Dermatology. 2021 Mar 1;238(2):347. doi:10.1159/000516138 PubMed PMID: 34091453.

10. Geskin LJ, Kim EJ, Angello JT, Kim YH. Evaluating the Treatment Patterns of Chlormethine/Mechlorethamine Gel in Patients With Stage I-IIA Mycosis Fungoides: By-time Reanalysis of a Randomized Controlled Phase 2 Study. Clin Lymphoma Myeloma Leuk. 2021 Feb 1;21(2):119-124.e4. doi:10.1016/j.clml.2020.11.022 PubMed PMID: 33358692.

11. Alberti-Violetti S, Ardigò M, Massone C, Pileri A, Sala R, Teoli M, et al. Effectiveness and tolerability of chlormethine gel for the management of mycosis fungoides: a multicenter real-life evaluation. Front Oncol. 2023;13:1298296. doi:10.3389/fonc.2023.1298296

12. Lessin SR, Duvic M, Guitart J, Pandya AG, Strober BE, Olsen EA, et al. Topical chemotherapy in cutaneous T-cell lymphoma: Positive results of a randomized, controlled, multicenter trial testing the efficacy and safety of a novel mechlorethamine, 0.02%, gel in mycosis fungoides. JAMA Dermatol. 2013 Jan;149(1):25–32. doi:10.1001/2013.jamadermatol.541 PubMed PMID: 23069814.

13. Querfeld C, Scarisbrick JJ, Assaf C, Guenova E, Bagot M, Ortiz-Romero PL, et al. Post hoc Analysis of a Randomized, Controlled, Phase 2 Study to Assess Response Rates with Chlormethine/Mechlorethamine Gel in Patients with Stage IA-IIA Mycosis Fungoides. Dermatology. 2022 Mar 1;238(2):347–57. doi:10.1159/000516138 PubMed PMID: 34091453.

14. Alexander-Savino C V., Chung CG, Gilmore ES, Carroll SM, Poligone B. Randomized Mechlorethamine/Chlormethine Induced Dermatitis Assessment Study (MIDAS) Establishes Benefit of Topical Triamcinolone 0.1% Ointment Cotreatment in Mycosis Fungoides. Dermatol Ther (Heidelb). 2022;12(3):643–54. doi:10.1007/s13555-022-00681-6

15. Gilmore ES, Alexander-Savino C V., Chung CG, Poligone B. Evaluation and management of patients with early-stage mycosis fungoides who interrupt or discontinue topical mechlorethamine gel because of dermatitis. JAAD Case Rep. 2020 Sep 1;6(9):878–81. doi:10.1016/j.jdcr.2020.05.031

16. Lessin SR, Duvic M, Guitart J, Pandya AG, Strober BE, Olsen EA, et al. Topical chemotherapy in cutaneous T-cell lymphoma: positive results of a randomized, controlled, multicenter trial testing the efficacy and safety of a novel mechlorethamine, 0.02%, gel in mycosis fungoides. JAMA Dermatol. 2013 Jan;149(1):25–32. doi:10.1001/2013.jamadermatol.541 PubMed PMID: 23069814.

17. Marchesi F, Turriziani M, Tortorelli G, Avvisati G, Torino F, De Vecchis L. Triazene compounds: mechanism of action and related DNA repair systems. Pharmacol Res. 2007 Oct;56(4):275–87. doi:10.1016/j.phrs.2007.08.003 PubMed PMID: 17897837.

18. Chang YT, Ignatova D, Hoetzenecker W, Pascolo S, Fassnacht C, Guenova E. Increased Chlormethine-Induced DNA Double-Stranded Breaks in Malignant T Cells from Mycosis Fungoides Skin Lesions. JID innovations : skin science from molecules to population health. 2022 Jan;2(1):100069. doi:10.1016/j.xjidi.2021.100069 PubMed PMID: 34977846.

19. Litterman AJ, Zellmer DM, Grinnen KL, Hunt MA, Dudek AZ, Salazar AM, et al. Profound impairment of adaptive immune responses by alkylating chemotherapy. J Immunol. 2013 Jun;190(12):6259–68. doi:10.4049/jimmunol.1203539 PubMed PMID: 23686484.

20. Litterman AJ, Dudek AZ, Largaespada DA. Alkylating chemotherapy may exert a uniquely deleterious effect upon neo-antigen-targeting anticancer vaccination. Oncoimmunology. 2013 Oct;2(10):e26294. doi:10.4161/onci.26294 PubMed PMID: 24251080.

21. Guenova E, Ortiz-Romero PL, Poligone B, Querfeld C. Mechanism of action of chlormethine gel in mycosis fungoides. Journal of the European Academy of Dermatology and Venereology. 2023;37(9):1739–48. doi:10.1111/jdv.19237 PubMed PMID: 37262305.

22. Kalliara E, Belfrage E, Gullberg U, Drott K, Ek S. Spatially Guided and Single Cell Tools to Map the Microenvironment in Cutaneous T-Cell Lymphoma. Cancers. 2023. doi:10.3390/cancers15082362

23. Pileri A, Guglielmo A, Grandi V, Violetti SA, Fanoni D, Fava P, et al. The Microenvironment's Role in Mycosis Fungoides and Sézary Syndrome: From Progression to Therapeutic Implications. Cells. 2021 Oct;10(10). doi:10.3390/cells10102780 PubMed PMID: 34685762.

24. Aliazis K, Christofides A, Shah R, Yeo YY, Jiang S, Charest A, et al. The tumor microenvironment's role in the response to immune checkpoint blockade. Nature Cancer. Nature Research; 2025. p. 924–37. doi:10.1038/s43018-025-00986-3 PubMed PMID: 40514448.

25. Wasmer MH, Krebs P. The Role of IL-33-Dependent Inflammation in the Tumor Microenvironment. Front Immunol. 2016;7:682. doi:10.3389/fimmu.2016.00682 PubMed PMID: 28119694.

26. Olsen EA, Whittaker S, Kim YH, Duvic M, Prince HM, Lessin SR, et al. Clinical end points and response criteria in mycosis fungoides and Sézary syndrome: A consensus statement of the International Society for Cutaneous Lymphomas, the United States Cutaneous Lymphoma Consortium, and the Cutaneous Lymphoma Task Force of the European Organisation for Research and Treatment of Cancer. Journal of Clinical Oncology. 2011. p. 2598–607. doi:10.1200/JCO.2010.32.0630 PubMed PMID: 21576639.

27. Davis MA, Kazmi SMS, Dunn AK. Imaging depth and multiple scattering in laser speckle contrast imaging. J Biomed Opt. 2014 Aug 4;19(8):086001. doi:10.1117/1.JBO.19.8.086001 PubMed PMID: 25089945.

28. Cracowski JL, Roustit M. Current Methods to Assess Human Cutaneous Blood Flow: An Updated Focus on Laser-Based-Techniques. Microcirculation. 2016 Jul 1;23(5):337–44. doi:10.1111/MICC.12257 PubMed PMID: 26607042.

29. Pauling JD, Shipley JA, Hart DJ, McGrogan A, McHugh NJ. Use of Laser Speckle Contrast Imaging to Assess Digital Microvascular Function in Primary Raynaud Phenomenon and Systemic Sclerosis: A Comparison Using the Raynaud Condition Score Diary. J Rheumatol. 2015 Jul 1;42(7):1163–8. doi:10.3899/JRHEUM.141437 PubMed PMID: 26034146.

30. Birkhoff W, de Vries J, Dent G, Verma A, Kerkhoffs JL, van Meurs AHF, et al. Retinal microcirculation imaging in sickle cell disease patients. Microvasc Res. 2018 Mar 1;116:1–5. doi:10.1016/j.mvr.2017.09.001 PubMed PMID: 28943261.

31. Mergen C, Wind S, Van Schaick M, Rousel J, Nadaban A, Rijneveld R, et al. Characterization of skin barrier function and ceramide composition in patients with mycosis fungoides. Eur J Cancer. 2023 Sep 1;190. doi:10.1016/j.ejca.2023.113050

32. Clark RA, Watanabe R, Teague JE, Schlapbach C, Tawa MC, Adams N, et al. Skin effector memory T cells do not recirculate and provide immune protection in alemtuzumab-treated CTCL patients. Sci Transl Med. 2012 Jan 18;4(117). doi:10.1126/scitranslmed.3003008 PubMed PMID: 22261031.

33. Watanabe R, Gehad A, Yang C, Scott LL, Teague JE, Schlapbach C, et al. Human skin is protected by four functionally and phenotypically discrete populations of resident and recirculating memory T cells. Sci Transl Med. 2015 Mar 18;7(279). doi:10.1126/scitranslmed.3010302 PubMed PMID: 25787765.

34. Hoppe RT, Medeiros LJ, Warnke RA, Wood GS. CD8-positive tumor-infiltrating lymphocytes influence the long-term survival of patients with mycosis fungoides. J Am Acad Dermatol. 1995;32(3):448–53. doi:10.1016/0190-9622(95)90067-5 PubMed PMID: 7868714.

35. Vermeer MH, van Doorn R, Dukers D, Bekkenk MW, Meijer CJ, Willemze R. CD8+ T cells in cutaneous T-cell lymphoma: expression of cytotoxic proteins, Fas Ligand, and killing inhibitory receptors and their relationship with clinical behavior. J Clin Oncol. 2001 Dec;19(23):4322–9. doi:10.1200/JCO.2001.19.23.4322 PubMed PMID: 11731515.

36. O'Malley JT, de Masson A, Lowry EL, Giobbie-Hurder A, LeBoeuf NR, Larocca C, et al. Radiotherapy eradicates malignant T cells and is associated with improved survival in early-stage mycosis fungoides. Clinical Cancer Research. 2020 Jan 15;26(2):408–18. doi:10.1158/1078-0432.CCR-18-4147 PubMed PMID: 31636100.

37. Galluzzi L, Senovilla L, Zitvogel L, Kroemer G. The secret ally: immunostimulation by anticancer drugs. Nat Rev Drug Discov. 2012 Feb;11(3):215–33. doi:10.1038/nrd3626 PubMed PMID: 22301798.

38. Hahtola S, Tuomela S, Elo L, Häkkinen T, Karenko L, Nedoszytko B, et al. Th1 response and cytotoxicity genes are down-regulated in cutaneous T-cell lymphoma. Clinical Cancer Research. 2006;12(16):4812–21. doi:10.1158/1078-0432.CCR-06-0532 PubMed PMID: 16914566.

39. Sugaya M, Tokura Y, Hamada T, Tsuboi R, Moroi Y, Nakahara T, et al. Phase II study of i.v. interferon-gamma in Japanese patients with mycosis fungoides. J Dermatol. 2014 Jan;41(1):50–6. doi:10.1111/1346-8138.12341 PubMed PMID: 24354781.

40. Vermeer BJ, Reman FC, Van Gent CM. The determination of lipids and proteins in suction blister fluid. Journal of Investigative Dermatology. 1979;73(4):303–5. doi:10.1111/1523-1747.ep12531833 PubMed PMID: 479634.

41. van Ruissen MCE, van Diemen M, Botros L, Tomljanovic I, Achbo H, Eleftheriou D, et al. Breaking Barriers: Characterization of the Intradermal Lipopolysaccharide Challenge as an In Vivo Model for Controlled Induction of Vascular Leakage in Healthy Volunteers. Clin Pharmacol Ther. 2025 Mar 1. doi:10.1002/cpt.70126

42. Ronner MN, Grievink HW, Saghari M, Osse M, van den Bosch TPP, Damman J, et al. Profiling a Neo-Antigen-Driven Immune Response in Healthy Volunteers: A Randomized, Double-Blind, Placebo-Controlled Study of the KLH Challenge Model. Clin Pharmacol Ther. 2025 Nov 1;118(5):1132–42. doi:10.1002/cpt.70007 PubMed PMID: 40696765.

43. Rojahn TB, Vorstandlechner V, Krausgruber T, Bauer WM, Alkon N, Bangert C, et al. Single-cell transcriptomics combined with interstitial fluid proteomics defines cell type–specific immune regulation in atopic dermatitis. Journal of Allergy and Clinical Immunology. 2020 Nov 1;146(5):1056–69. doi:10.1016/j.jaci.2020.03.041 PubMed PMID: 32344053.

44. Guenova E, Watanabe R, Teague JE, Desimone JA, Jiang Y, Dowlatshahi M, et al. TH2 cytokines from malignant cells suppress TH1 responses and enforce a global TH2 bias in leukemic cutaneous T-cell lymphoma. Clin Cancer Res. 2013 Jul;19(14):3755–63. doi:10.1158/1078-0432.CCR-12-3488 PubMed PMID: 23785046.

45. Alexander-Savino C V, Chung CG, Gilmore ES, Carroll SM, Poligone B. Randomized Mechlorethamine/Chlormethine Induced Dermatitis Assessment Study (MIDAS) Establishes Benefit of Topical Triamcinolone 0.1% Ointment Cotreatment in Mycosis Fungoides. Dermatol Ther (Heidelb). 2022 Mar;12(3):643–54. doi:10.1007/s13555-022-00681-6 PubMed PMID: 35122614.

597 TABLES

598 **Table 1. Demographics, patient, and treatment characteristics.**

599

CHARACTERISTICS	MF PATIENTS (N=17)		HEALTHY CONTROLS (N=10)
Age, years			
Mean (SD, range)	52.6 (15.2, 19–72)		54.2 (18.2, 22–73)
Sex, N (%)			
Female	7 (41.2)		5 (50.0)
Male	10 (58.8)		5 (50.0)
Fitzpatrick skin type, N (%)			
I	2 (11.8)		0
II	12 (70.6)		4 (40.0)
III	2 (11.8)		6 (60.0)
IV	0		0
V	1 (5.9)		0
VI	0		0
Sampling location, N (%)			
Trunk	6 (35.3)		4 (40.0)
Swimsuit area	4 (23.5)		3 (30.0)
Upper leg	5 (29.4)		2 (20.0)
Lower leg	2 (11.8)		1 (10.0)
MF stage, N (%)			NA
IA	13 (76.5)		
IB	4 (23.5)		
Target lesion, N (%)			NA
Patch	14 (82.4)		
Plaque	3 (17.6)		
CAILS, mean (SD, range)	**Baseline**	**Post-treatment**	NA
Total (n=17)	16.5 (3.5, 9-22)	11.6 (4.4, 4-18)	
Fast responder (n=3)	17.3 (3.7, 13-22)	5.0 (1.0, 4-6)	
Intermediate responder (n=4)	17.8 (5.1, 9-22)	9.0 (2.8, 5-12)	
Slow responder (n=4)	15.5 (2.9, 12-20)	11.3 (2.2, 10-15)	
Non responder (n=6)	15.8 (1.2, 14-18)	16.2 (1.6, 14-18)	
mCAILS, mean (SD, range)	**Baseline**	**Post-treatment**	NA
Total (n=17)	15.1 (3.3, 8-20)	10.1 (4.3, 0-17)	
Fast responder (n=3)	14.3 (1.7, 12-16)	3.5 (0.5, 0-4)	
Intermediate responder (n=4)	16.8 (5.1, 8-20)	7.7 (2.6, 4-10)	
Slow responder (n=4)	14.5 (3.6, 10-20)	9.8 (2.1, 8-13)	
Non responder (n=6)	14.6 (1.0, 13-16)	14.6 (1.6, 13-17)	
mSWAT, mean (SD, range)	**Baseline**	**Post-treatment**	NA
Total (n=17)	12.5 (17.2, 2-79)	10.1 (15.7, 3-71)	
Fast responder (n=3)	9.7 (5.6, 2-15)	6.3 (2.9, 3-10)	
Intermediate responder (n=4)	6.3 (1.3, 5-8)	3.8 (0.4, 3-4)	
Slow responder (n=4)	26.3 (30.1, 4-79)	21.5 (28.6, 3-71)	
Non responder (n=6)	9.0 (4.0, 4-16)	8.5 (4.5, 3-16)	

Days of treatment application*, mean (range)		NA
Total, n=15	68.0 (23-100)	
Fast responder (n=3)	39.0 (23-51)	
Intermediate responder (n=3)	65.3 (30-88)	
Slow responder (n=4)	69.3 (58-89)	
Non responder (n=5)	86.0 (61-100)	
Compliance % (range)		NA
Total (n=16)	89.9 (50.0-100)	
Fast responder (n=3)	99.2 (97.7-100)	
Intermediate responder (n=4)	89.4 (83.0-95.3)	
Slow responder (n=4)	87.9 (72.3-98.4)	
Non responder (n=6)	86.2 (50.0-97.1)**	
Duration of dermatitis in days (mean, range)		NA
Total, n=16	15.6 (0-87)	
Fast responder (n=3)	43.0 (0-87)	
Intermediate responder (n=4)	17.3 (0-53)	
Slow responder (n=4)	9.3 (4-16)	
Non responder (n=5)	11.3 (0-14)**	
Time to first dermatitis reaction, mean in weeks (range)		NA
Total (n=12***)	5.4 (0.5-13.5)	
Fast responder (n=3)	4.9 (3.8-5.8)	
Intermediate responder (n=3****)	3.8 (1.0-7.8)	
Slow responder (n=4)	8.4 (5.5-13.5)	
Non responder (n=2*****)	2.8 (0.5-5.0)	

*Total of 95 days of treatment application in case no application site reaction occurred. Ohterwise treatment application frequency was down-titrated following table S1. Early drop-outs were left out of the days of treatment application.

** 1 patient applied 61 days of treatment instead of the advised 46 days, this patient was left out mean % compliance of non-responders and mean duration of dermatitis in days in non-responders.

*** 5 patients out of the total 17 patients did not experience a dermatitis reaction and were left out of the mean and range of Time to first dermatitis reaction, total.

**** 1 patient experienced no dermatitis reaction and was left out of the mean and range of Time to first dermatitis reaction, intermediate responder.

***** 4 patients experienced no dermatitis reaction and were left out of the mean and range of Time to first dermatitis reaction, non responder.

FIGURE LEGENDS

Figure 1. Study design. MF patients (stage 1A-1B) were included after topical CTCL treatments had been discontinued for 8 weeks and systemic CTCL treatments had been discontinued for 10-18 weeks, depending on the time required to reach 5 half-lives, prior to the baseline week 0 visit. 21 Patients and 11 healthy controls participated in the observational study of 6 weeks; all 21 patients continued in the open-label interventional part where they applied topical chlormethine for 16 weeks on all MF lesions excluding the face. Biopsies and suction blisters were drawn at the end of the observational part from healthy controls, from patients of a representative MF lesion and a contralateral non-lesional skin site. After 16 weeks of treatment, a suction blister was drawn from the same MF lesion. If a chlormethine-induced dermatitis reaction during treatment occurred, optional sampling of the respective lesion was performed.

[1] At baseline, sampling was performed of lesional skin and contralateral non-lesional skin.

[2] *After 16 weeks of treatment, the same treated lesion was resampled.*

Created with BioRender.com.

Figure 2. Chlormethine induces heterogeneous early clinical responses using mCAILS, treatment-associated dermatitis correlates with clinical response, and baseline cytotoxic immune environment distinguishes responders. (A) clinical photographs and laser speckle contrast imaging depicting microcirculation per response group. (B) mCAILS at baseline and at 16W of treatment per response group. P-values indicated: <0.05=*, <0.01=**, <0.001=***, <0.0001=****. (C) Change from baseline in mCAILS at 16 weeks and total days of dermatitis suction correlated significantly using Spearman correlation (r=0.60, p<0.01). (D) Responders showed significantly elevated activated cytotoxic T-cells at baseline, whereas non-responders did not. FR, fast responder; IR, intermediate responder; SR, slow responder; NR, non-responder; LSCI, laser speckle contrast imaging; mCAILS, modified composite assessment of index lesion severity; CFB, change from baseline.

Figure 3. Responders exhibit reduction in dominant T-cell clones and T-cell clonal diversity. (A) Number of unique clones for 2 fast responders (FR), 1 intermediate responder (IR) and 4 non-responders (NR) at baseline and after 16 weeks of treatment. Responders demonstrate a consistent reduction in unique clones. (B) The effectiveness of chlormethine treatment is demonstrated in an intermediate responder by the reduced top clone and reduced T-cell clonal diversity after 16 weeks of chlormethine treatment. The diversity decreased from 391 to 142 unique T-cell clones. (C) The non-responder showed a decrease of diverse clones (from 206 to 29), however no decrease in the top clone after 16 weeks of treatment. In both intermediate responder and non-responder the number of persistent clones was relatively low (15 and 4 respectively).

Figure 4. Clinical response associates with composition of the immune infiltrate; visualization of the tumor microenvironment in responders and non-responders using Imaging mass cytometry (IMC). (A) Representative IMC images of a responder (top) and non-responder (bottom), comparing baseline (left) and treated samples (right). Overview panels show cellular infiltration with keratin (white, epidermis), CD68 (lime) macrophages, CD11b (yellow) myeloid lineage, and CD3 (blue) and CD7 (red) marking T cells. The responder exhibits a $CD4^{-}CD8^{-}CD7^{-}CD3^{+}$ tumor phenotype, whereas the non-responder shows a $CD4^{+}CD8^{-}CD7^{-}CD3^{+}$ phenotype. T-cell panels highlight $CD8^{+}$ (magenta) T cells, $CD4^{+}$ (cyan) T cells, and tumor T cells (blue in responder; cyan in non-responder). The myeloid compartment is displayed with CD1a (cyan), CD11c (magenta), CD11b (yellow), and CD14 (red). (B) Absolute IMC immune cell abundance (mean counts/mm² per patient) in non-responders (baseline, NRB; treated, NRT) and responders (baseline, RB; treated, RT). Cell counts remain stable or increase in non-responders but markedly decrease in responders, consistent with (A). (C) Absolute abundance of individual immune cell

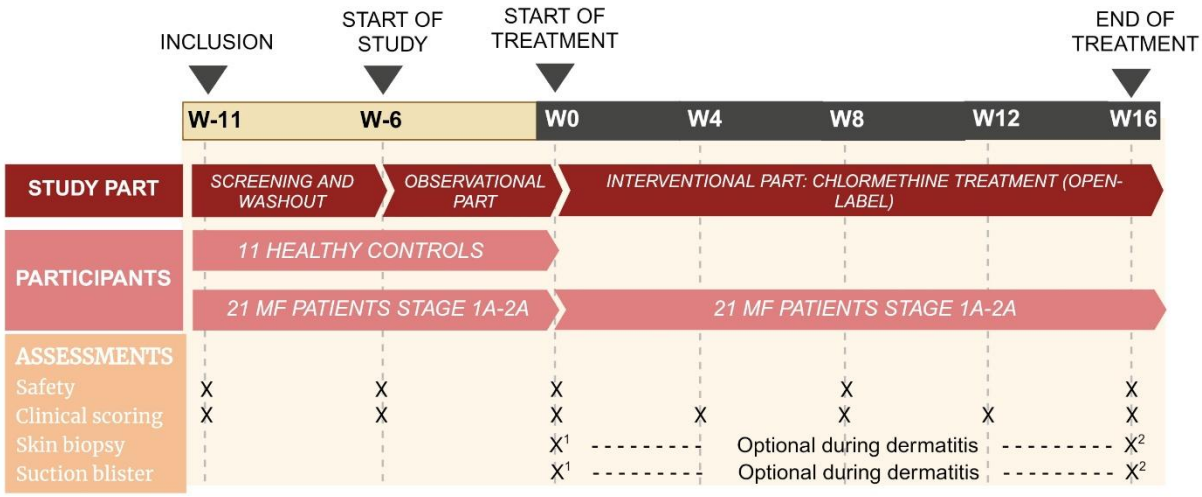
subsets shows a consistent pattern across all cell types, mirroring (B). (D) Absolute abundance of $CD4^+$ and $CD8^+$ T cells, with $CD4^+$ and $CD4^-$ tumor populations separated (based on clinical annotation) to distinguish tumor-containing versus reactive compartments. Abbreviations: NRB, non-responders baseline; NRT, non-responders treated; RB, responders baseline; RT, responders treated; γδ T cells, gamma delta T cells; DCs, dendritic cells; ILCs, innate lymphoid cells; $mCD14^+CD68^+$, myeloid $CD14^+CD68^+$ cells; $mCD14^+CD68^-$, myeloid $CD14^+CD68^-$ cells.

Figure 5. Clinical response to chlormethine treatment is accompanied by contraction of inflammatory and immunosuppressive cells using flow cytometry of suction blister interstitial fluid. Data are presented as median with interquartile range, and whiskers represent minimum and maximum. Statistical significance was derived from Wilcoxon matched-pairs signed rank test and corrected using the Holm–Šídák method. *p<0.05. FR, fast responder; IR, intermediate responder; SR, slow responder. NL, non-lesional control skin, L W0, lesional skin at baseline, L W16, lesional skin after 16 weeks of chlormethine treatment.

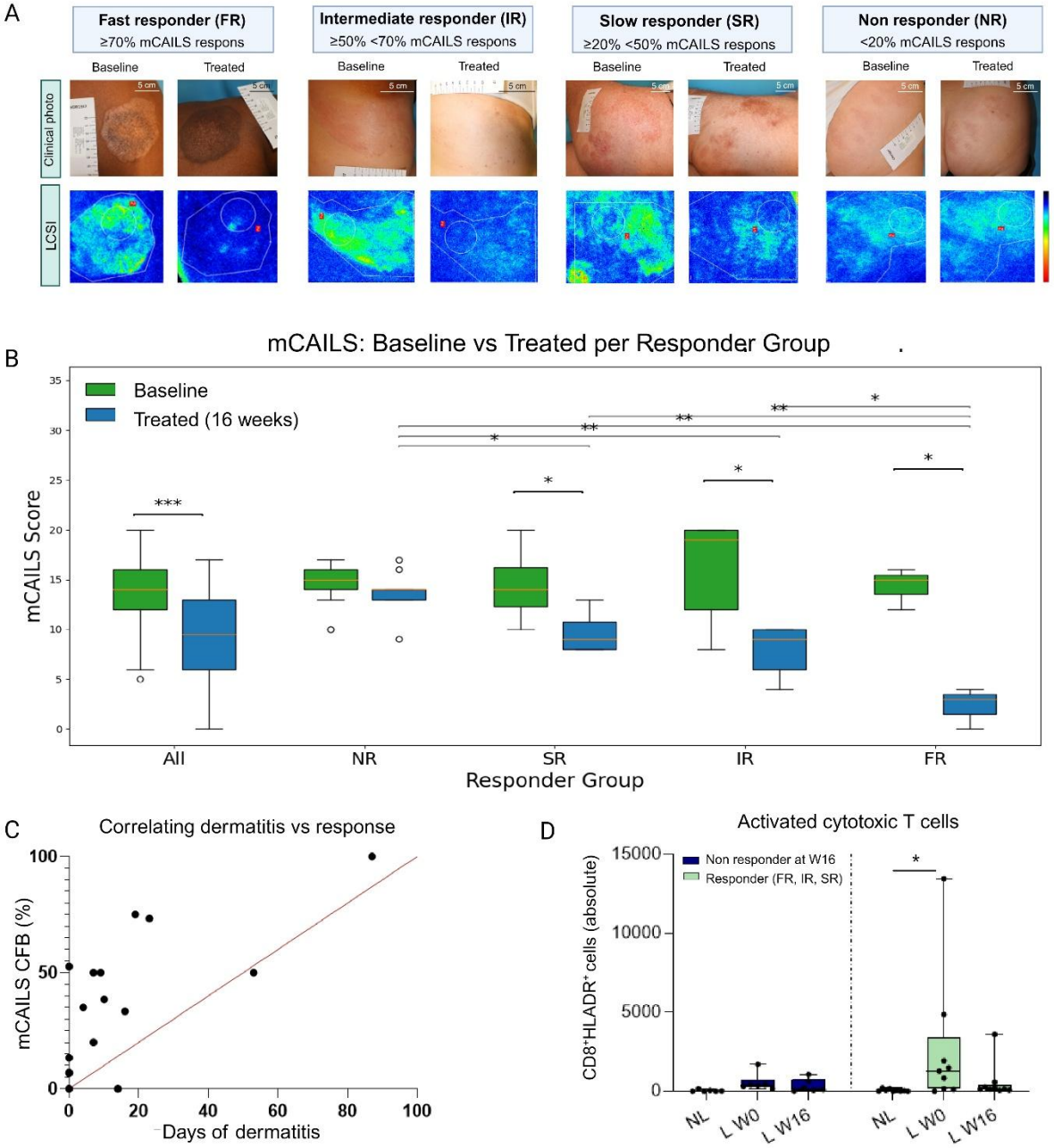
Figure 6. Blister-fluid proteomics reveals extensive baseline lesional dysregulation and response-associated remodeling after chlormethine. (A) Forest plot showing 43 differentially expressed proteins (29 unique across panels) in lesional skin after 16 weeks of chlormethine treatment relative to baseline. Points represent linear mixed-effects model estimates with 95% confidence intervals, corrected for multiple testing using the Benjamini-Hochberg (BH) correction. Positive values indicate higher abundance after treatment. Significance was defined as p-adjusted<0.05. (B) Boxplots showing the normalized protein expression (NPX) of selected inflammatory and checkpoint proteins across healthy control baseline, non-lesional control baseline, lesional baseline and lesional samples after 16 weeks of chlormethine treatment. Statistical significance was derived from linear mixed-effects models with BH correction. *p<0.05, **p<0.01, ***p<0.001. (C) Heatmap showing a subset of 13 significant proteins (11 unique across panels, p-adjusted<0.01) out of 43 significant proteins (39 unique across panels, BH-corrected, p-adjusted p<0.05) comparing lesional baseline samples from responders to non-responders. Protein expression (NPX) is shown as scaled values (z-scores), with red indicating higher and gray lower relative abundance. (D) Principal component analysis (PCA) of blister fluid proteomes from all samples colored by response group. Samples separate along PC1 in a gradient from healthy control and non-lesional skin (right) toward dermatitis and baseline lesional samples (left), with treated samples distributed in between. This suggests a continuum of inflammatory states that aligns with graded clinical response groups. (E) Heatmap of a subset of 27 significant proteins (22 unique across panels, p-adjusted<0.01) out of 52 significant proteins (42 unique across panels, BH-corrected, p-adjusted p<0.05) from the comparison of responders to non-

responders in treated samples (NPX z-scores). Red indicates high relative expression, gray indicates low relative expression.

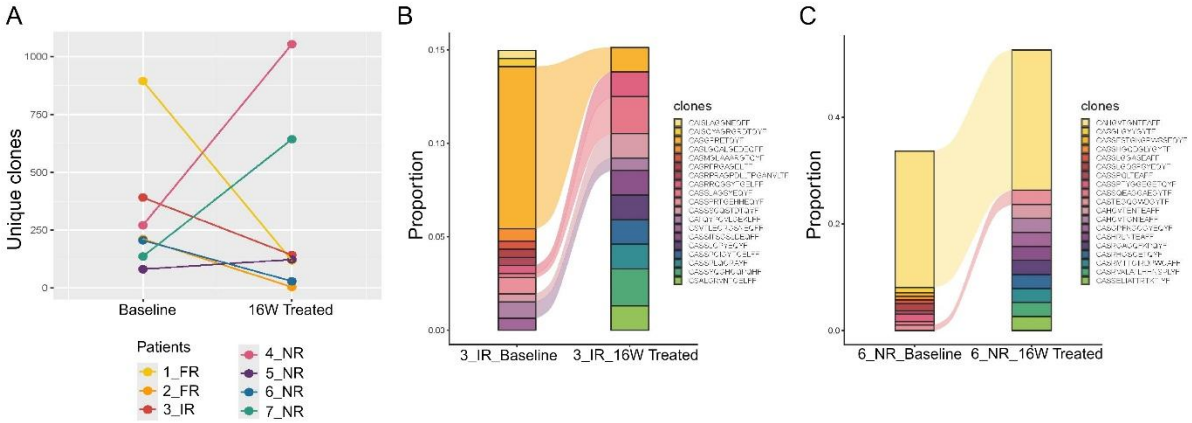
Figure 7. Dermatitis samples display heightened immune activation and an inflammation-high soluble profile. (A) IMC imaging of a dermatitis lesion from a responder ($CD4^{-}CD8^{+}$ tumor type). The left panel presents a 1 mm² tissue overview highlighting keratin (white), αSMA (red), CD20 (yellow), CD3 (cyan), and CD14 (magenta) to illustrate tissue architecture and immune infiltration. The right panels show zoomed views: the upper panel focuses on T cells (keratin, CD4, CD8a, CD3, CD7), and the lower panel on myeloid cells (CD11b, CD1a, CD14, CD11c). (B) IMC heatmap of key immune cell phenotypes across five patients with chlormethine-induced dermatitis. Scaled counts (z-scores) reflect relative abundance in dermatitis, baseline, and treated samples, with peaks during dermatitis reactions and declines after treatment. (C) Forest plot depicting 25 differentially expressed proteins (21 unique across panels) in dermatitis versus lesional skin at baseline. Points represent linear mixed-effect model estimates with 95% confidence intervals; multiple testing correction was applied using the Benjamini-Hochberg (BH) method. Positive values indicate higher abundance during dermatitis. Statistical significance was defined as p-adjusted<0.05. (D) Forest plot displaying 75 differentially expressed proteins (54 unique across panels) in dermatitis versus treated samples. Linear mixed-effects model estimates are shown with 95% confidence intervals (BH-corrected); positive values indicate higher abundance during dermatitis (p-adjusted<0.05). (E) Boxplots showing the normalized protein expression (NPX) for selected inflammatory and cytotoxic proteins across lesional baseline, dermatitis and lesional samples after 16 weeks of chlormethine treatment. Statistical significance was derived from linear mixed-effects models with BH correction. *p<0.05, **p<0.01, ***p<0.001. Abbreviations: ASR, application site reactions, dermatitis in the clinical context; NR, non-responder; R, responder; γδ T cells, gamma delta T cells; ILCs, innate lymphoid cells; $mCD14^{+}CD68^{+}$, myeloid $CD14^{+}CD68^{+}$ cells; DCs, dendritic cells; $mCD14^{+}CD68^{-}$, myeloid $CD14^{+}CD68^{-}$ cells.


INCLUSION
START OF STUDY
START OF TREATMENT
END OF TREATMENT
W-11
W-6
W0
W4
W8
W12
W16
STUDY PART
SCREENING AND WASHOUT
OBSERVATIONAL PART
INTERVENTIONAL PART: CHLORMETHINE TREATMENT (OPEN-LABEL)
PARTICIPANTS
11 HEALTHY CONTROLS
21 MF PATIENTS STAGE 1A-2A
21 MF PATIENTS STAGE 1A-2A
ASSESSMENTS
Safety
Clinical scoring
Skin biopsy
Suction blister
Optional during dermatitis
Optional during dermatitis

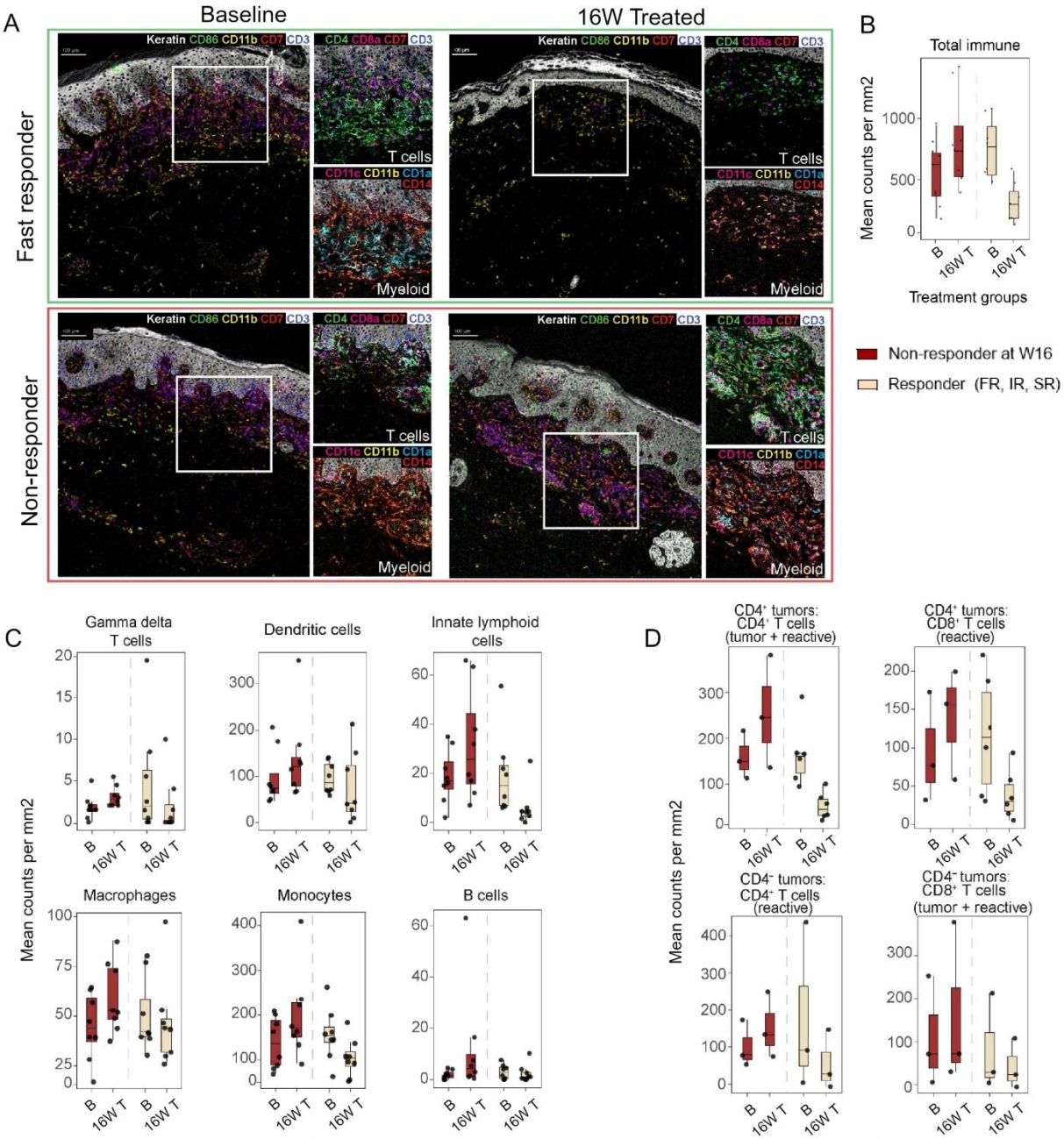
716


A
Fast responder (FR)
≥70% mCAILS respons
Intermediate responder (IR)
≥50% <70% mCAILS respons
Slow responder (SR)
≥20% <50% mCAILS respons
Non responder (NR)
<20% mCAILS respons
Baseline
Treated
Clinical photo
LCSI
B
mCAILS: Baseline vs Treated per Responder Group
Baseline
Treated (16 weeks)
mCAILS Score
All
NR
SR
IR
FR
Responder Group
C
Correlating dermatitis vs response
mCAILS CFB (%)
Days of dermatitis
D
Activated cytotoxic T cells
Non responder at W16
Responder (FR, IR, SR)
CD8+HLADR+ cells (absolute)
NL
L W0
L W16

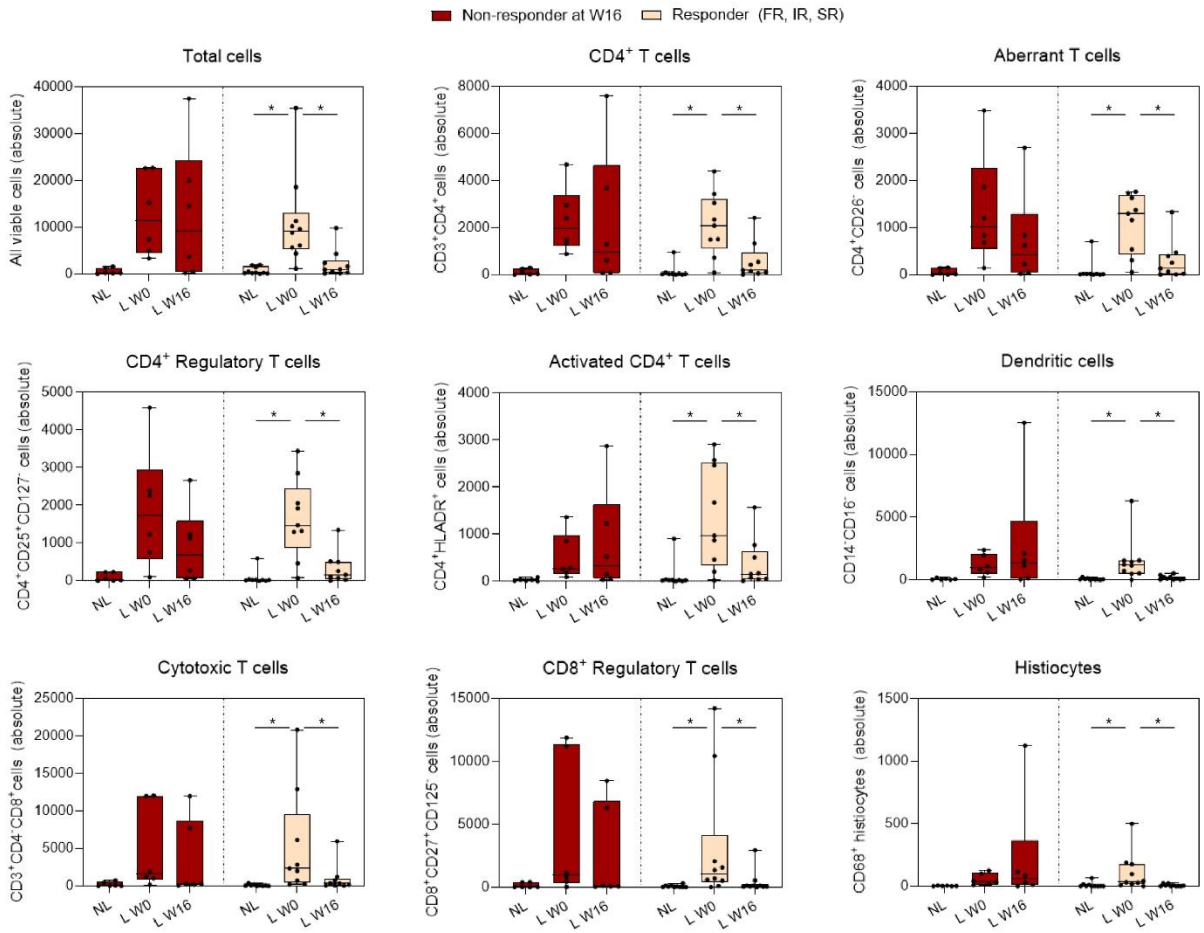
717


A
Unique clones
1000
750
500
250
0
Baseline
16W Treated
Patients
1_FR
2_FR
3_IR
4_NR
5_NR
6_NR
7_NR
B
Proportion
0.15
0.10
0.05
0.00
clones
3_IR_Baseline
3_IR_16W Treated
C
Proportion
0.4
0.2
0.0
clones
6_NR_Baseline
6_NR_16W Treated

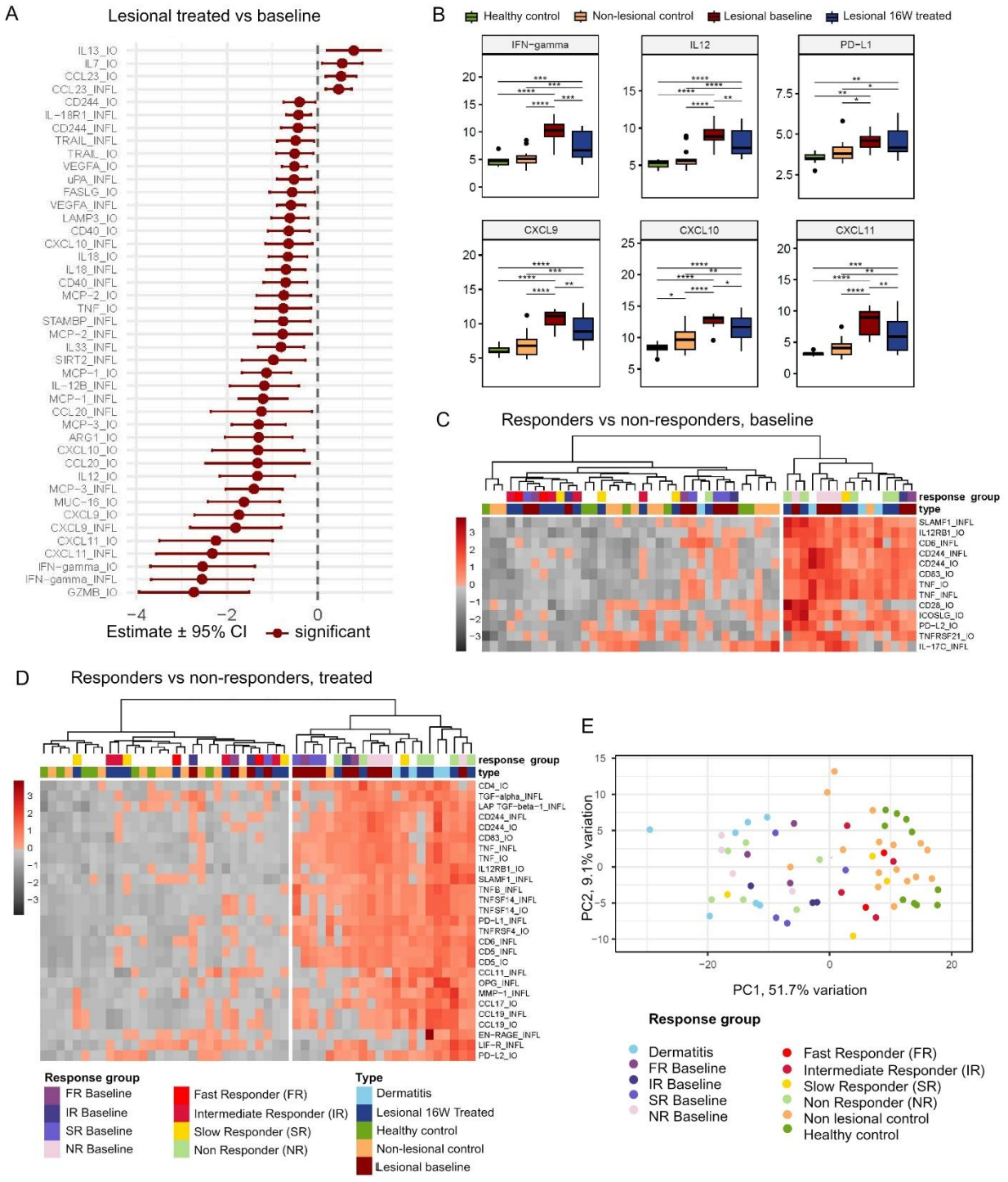
718


A
Baseline
16W Treated
Fast responder
Non-responder
Keratin CD86 CD11b CD7 CD3
CD4 CD8a CD7 CD3
T cells
CD11c CD11b CD1a CD14
Myeloid
B
Total immune
Mean counts per mm2
1000
500
0
B
16W T
Treatment groups
Non-responder at W16
Responder (FR, IR, SR)
C
Gamma delta T cells
Dendritic cells
Innate lymphoid cells
Macrophages
Monocytes
B cells
Mean counts per mm2
D
CD4+ tumors: CD4+ T cells (tumor + reactive)
CD4+ tumors: CD8+ T cells (reactive)
CD4- tumors: CD4+ T cells (reactive)
CD4- tumors: CD8+ T cells (tumor + reactive)

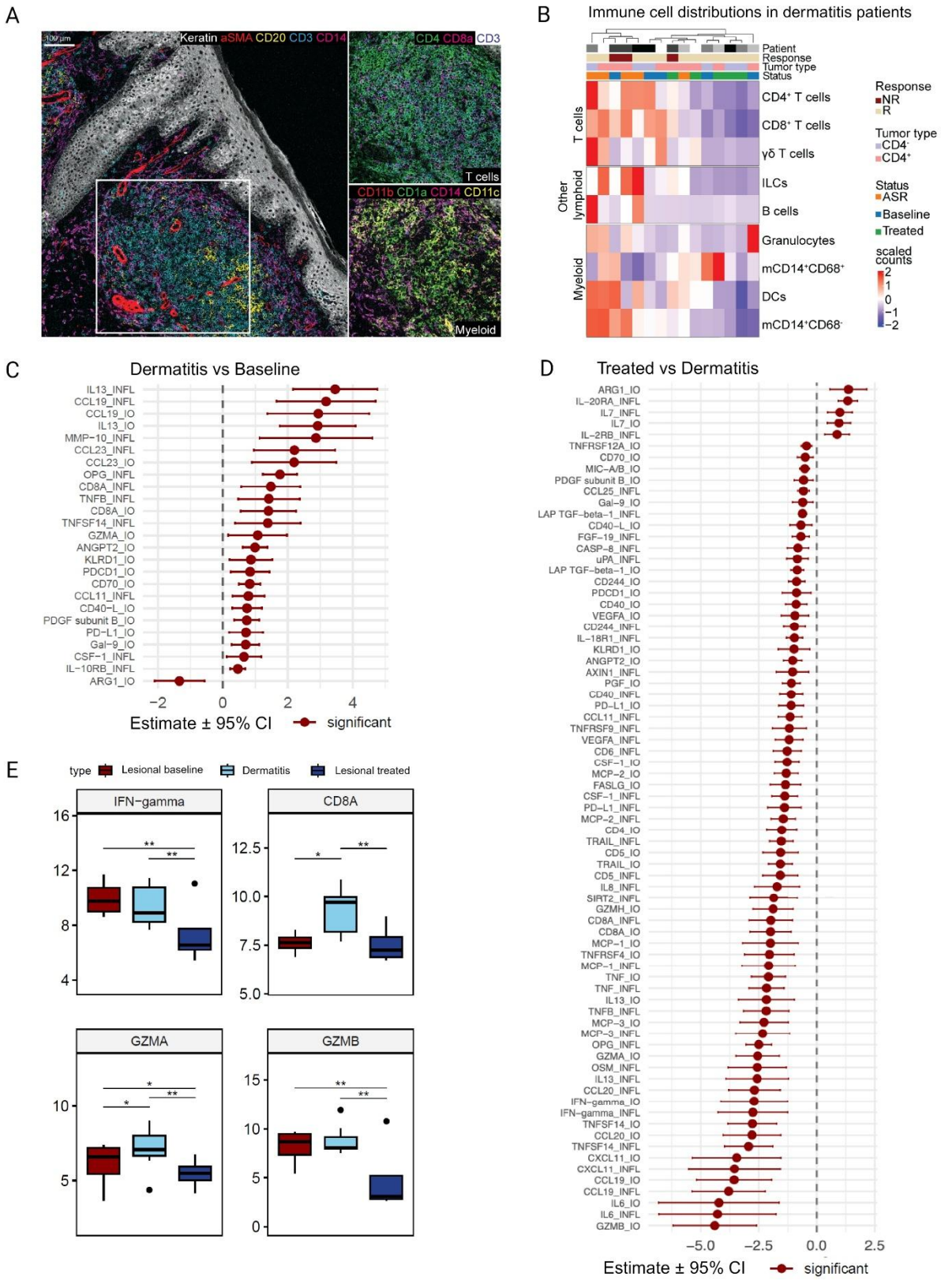
719


Non-responder at W16
Responder (FR, IR, SR)
Total cells
All viable cells (absolute)
CD4+ T cells
CD3+CD4+ cells (absolute)
Aberrant T cells
CD4+CD26- cells (absolute)
CD4+ Regulatory T cells
CD4+CD25+CD127- cells (absolute)
Activated CD4+ T cells
CD4+HLADR+ cells (absolute)
Dendritic cells
CD14-CD16- cells (absolute)
Cytotoxic T cells
CD3+CD4-CD8+ cells (absolute)
CD8+ Regulatory T cells
CD8+CD27+CD125- cells (absolute)
Histiocytes
CD68+ histiocytes (absolute)
NL
L W0
L W16

720


A
Lesional treated vs baseline
IL13_IO
IL7_IO
CCL23_IO
CCL23_INFL
CD244_IO
IL-18R1_INFL
CD244_INFL
TRAIL_INFL
TRAIL_IO
VEGFA_IO
uPA_INFL
FASLG_IO
VEGFA_INFL
LAMP3_IO
CD40_IO
CXCL10_INFL
IL18_IO
IL18_INFL
CD40_INFL
MCP-2_IO
TNF_IO
STAMBP_INFL
MCP-2_INFL
IL33_INFL
SIRT2_INFL
MCP-1_IO
IL-12B_INFL
MCP-1_INFL
CCL20_INFL
MCP-3_IO
ARG1_IO
CXCL10_IO
CCL20_IO
IL12_IO
MCP-3_INFL
MUC-16_IO
CXCL9_IO
CXCL9_INFL
CXCL11_IO
CXCL11_INFL
IFN-gamma_IO
IFN-gamma_INFL
GZMB_IO
−4
−2
0
Estimate ± 95% CI
significant
B
Healthy control
Non-lesional control
Lesional baseline
Lesional 16W treated
IFN-gamma
IL12
PD-L1
CXCL9
CXCL10
CXCL11
C
Responders vs non-responders, baseline
response group
type
SLAMF1_INFL
IL12RB1_IO
CD6_INFL
CD244_INFL
CD244_IO
CD83_IO
TNF_IO
TNF_INFL
CD28_IO
ICOSLG_IO
PD-L2_IO
TNFRSF21_IO
IL-17C_INFL
D
Responders vs non-responders, treated
response group
type
CD4_IO
TGF-alpha_INFL
LAP.TGF-beta-1_INFL
CD244_INFL
CD244_IO
CD83_IO
TNF_INFL
TNF_IO
IL12RB1_IO
SLAMF1_INFL
TNFB_INFL
TNFSF14_INFL
TNFSF14_IO
PD-L1_INFL
TNFRSF4_IO
CD6_INFL
CD5_INFL
CD5_IO
CCL11_INFL
OPG_INFL
MMP-1_INFL
CCL17_IO
CCL19_INFL
CCL19_IO
EN-RAGE_INFL
LIF-R_INFL
PD-L2_IO
Response group
FR Baseline
IR Baseline
SR Baseline
NR Baseline
Fast Responder (FR)
Intermediate Responder (IR)
Slow Responder (SR)
Non Responder (NR)
Type
Dermatitis
Lesional 16W Treated
Healthy control
Non-lesional control
Lesional baseline
E
PC2, 9.1% variation
PC1, 51.7% variation
Response group
Dermatitis
FR Baseline
IR Baseline
SR Baseline
NR Baseline
Fast Responder (FR)
Intermediate Responder (IR)
Slow Responder (SR)
Non Responder (NR)
Non lesional control
Healthy control

721


A
Keratin aSMA CD20 CD3 CD14
CD4 CD8a CD3
T cells
CD11b CD1a CD14 CD11c
Myeloid
B
Immune cell distributions in dermatitis patients
Patient
Response
Tumor type
Status
T cells
Other lymphoid
Myeloid
CD4⁺ T cells
CD8⁺ T cells
γδ T cells
ILCs
B cells
Granulocytes
mCD14⁺CD68⁺
DCs
mCD14⁺CD68⁻
Response
NR
R
Tumor type
CD4⁻
CD4⁺
Status
ASR
Baseline
Treated
scaled counts
2
1
0
−1
−2
C
Dermatitis vs Baseline
IL13_INFL
CCL19_INFL
CCL19_IO
IL13_IO
MMP−10_INFL
CCL23_INFL
CCL23_IO
OPG_INFL
CD8A_INFL
TNFB_INFL
CD8A_IO
TNFSF14_INFL
GZMA_IO
ANGPT2_IO
KLRD1_IO
PDCD1_IO
CD70_IO
CCL11_INFL
CD40−L_IO
PDGF subunit B_IO
PD−L1_IO
Gal−9_IO
CSF−1_INFL
IL−10RB_INFL
ARG1_IO
−2
0
2
4
Estimate ± 95% CI
significant
D
Treated vs Dermatitis
ARG1_IO
IL−20RA_INFL
IL7_INFL
IL7_IO
IL−2RB_INFL
TNFRSF12A_IO
CD70_IO
MIC−A/B_IO
PDGF subunit B_IO
CCL25_INFL
Gal−9_IO
LAP TGF−beta−1_INFL
CD40−L_IO
FGF−19_INFL
CASP−8_INFL
uPA_INFL
LAP TGF−beta−1_IO
CD244_IO
PDCD1_IO
CD40_IO
VEGFA_IO
CD244_INFL
IL−18R1_INFL
KLRD1_IO
ANGPT2_IO
AXIN1_INFL
PGF_IO
CD40_INFL
PD−L1_IO
CCL11_INFL
TNFRSF9_INFL
VEGFA_INFL
CD6_INFL
CSF−1_IO
MCP−2_IO
FASLG_IO
CSF−1_INFL
PD−L1_INFL
MCP−2_INFL
CD4_IO
TRAIL_INFL
CD5_IO
TRAIL_IO
CD5_INFL
IL8_INFL
SIRT2_INFL
GZMH_IO
CD8A_INFL
CD8A_IO
MCP−1_IO
TNFRSF4_IO
MCP−1_INFL
TNF_IO
TNF_INFL
IL13_IO
TNFB_INFL
MCP−3_IO
MCP−3_INFL
OPG_INFL
GZMA_IO
OSM_INFL
IL13_INFL
CCL20_INFL
IFN−gamma_IO
IFN−gamma_INFL
TNFSF14_IO
CCL20_IO
TNFSF14_INFL
CXCL11_IO
CXCL11_INFL
CCL19_IO
CCL19_INFL
IL6_IO
IL6_INFL
GZMB_IO
−5.0
−2.5
0.0
2.5
Estimate ± 95% CI
significant
E
type
Lesional baseline
Dermatitis
Lesional treated
IFN−gamma
CD8A
GZMA
GZMB

722

Supplementary Files

This is a list of supplementary files associated with this preprint. Click to download.

- SupplementalMaterialCancerImmunologyImmunotherapy.docx
- CoverArtVisualAbstract.jpeg